Lightweight broadband microwave absorbing metamaterial with CB-ABS composites fabricated by 3D printing

Meng-Zhou Chen(陈孟州)[1], Liu-Ying Wang(汪刘应)[1,†], Gu Liu(刘顾)[1], Chao-Qun Ge(葛超群)[1], Di-Chen Li(李涤尘)[2], and Qing-Xuan Liang(梁庆宣)[2]

[1] *Xi'an Research Institute of High Technology, Xi'an* 710025, *China*

[2] *State Key Laboratory for Manufacturing Systems Engineering, Xi'an Jiaotong University, Xi'an* 710049, *China*

(Received 31 July 2022; revised manuscript received 4 September 2022; accepted manuscript online 21 September 2022)

The self-similarity, high geometric symmetry and spatial utilization properties of fractal structures provide new methods for the development of absorbing metamaterials. In this paper, the microwave absorption properties of the gradient dendritic fractal metamaterial structure (GDFMs) based on carbon black and acrylonitrile–butadiene–styrene composites were investigated. The optimal metamaterial structure has an effective absorption in the frequency range of 4.5–40 GHz. The rotational-symmetry GDFMs leads to the polarization independence, and the GDFMs exhibits a wide-angle absorption performance for both TE and TM waves. It is expected that the proposed GDFMs has good application prospects in electromagnetic wave absorption.

Keywords: additive manufacturing, broadband absorbing, polarization and angle independence, gradient dendritic fractal structure

PACS: 81.05.U–, 78.67.Pt, 07.57.–c, 42.25.Bs **DOI:** 10.1088/1674-1056/ac935c

1. Introduction

In recent years, electromagnetic absorbing metamaterials have been investigated and developed due to their extensive applications in many fields, such as stealth technology, electromagnetic pollution reduction and wireless communication.[1–5] Although conventional absorbing metamaterials could realize perfect absorption at a single frequency point, the narrow band absorption limits their applications.[6] Therefore, more and more research studies on broadband absorbing metamaterials have emerged, and many broadband methods have been proposed.[7–13] Duan *et al.*[14] proposed a gradient composite metastructure to achieve a −10 dB absorbing bandwidth in a wide frequency range. Zhou *et al.*[15] investigated a two-layer periodic stepped radar absorbing structure with ultra-broadband absorption performance, while Yang *et al.*[16] presented a design for a multilayer metamaterial and adjusted the geometric parameters and the distribution of spherical carbonyl iron powder to achieve broadband absorption. However, these methods do have some defects in spite of achieving broadband absorption. For instance, the multilayer structure will lead to a large thickness,[16] while the metamaterials containing magnetic materials usually result in an increase in density.[14,17–19] Furthermore, it is difficult to achieve broadband absorption and polarization and angle insensitivity simultaneously.[20–22]

The dendritic structure is a fractal structure with high geometric symmetry, which is isotropic to incident electromagnetic waves at different angles,[23] while gradient structure can not only achieve better impedance matching characteristics, but also significantly enhances the edge diffraction effect.[24,25] Therefore, the combination of dendritic structure and gradient structure can provide an effective way to design broadband absorbing metamaterials. Compared with the traditional manufacturing process, 3D printing technology can realize the efficient and precise fabrication of complex structures.[25,26]

In this work, a novel absorbing metamaterial based on the gradient dendritic fractal structure with broadband, polarization-independent and angle-insensitive characteristics was proposed. A gradient dendritic fractal metamaterial structure (GDFMs) based on carbon black and acrylonitrile–butadiene–styrene (CB-ABS) composites was successfully fabricated by fused deposition modelling (FDM) of 3D printing. The simulated and experimental results showed that a broadband absorption spectrum could be obtained. The wave absorption mechanism was also studied by analyzing the electromagnetic field and energy loss distributions.

2. Simulation and experiments

Figure 1 shows a schematic of the GDFMs. The unitary structure consists of the gradient dendritic structure and an outer circular structure. The eight-branch dendritic structure is composed of one three-stage V-structure rotated in 45° steps around the apex of the main branch of the structure. And the dendritic structure has gradient variations with respect to the primary level structure. The height and length of the primary level structure were H and L, while the width was W. Respectively, the gradient ratios were k, m and t. The structural

†Corresponding author. E-mail: lywangxa@163.com

© 2023 Chinese Physical Society and IOP Publishing Ltd

parameters of the secondary and third level structure were as follows: $L_2 = Lt$, $H_2 = Hk$, $W_2 = Wm$; $L_3 = Lt^2$, $H_3 = Hk^2$, $W_3 = Wm^2$. In addition, the height and width of the outer circular structure were H and D. The commercial software CST Microwave Studio was used for the numerical simulation. The unit cell boundary conditions were used in the x and y directions, and the open boundary condition was set in the z direction.

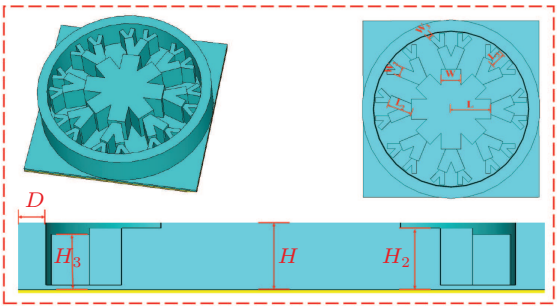


Fig. 1. Schematic diagram of the unit cell.

For the experiment, a vector network analyzer (Ceyear 3672C, China) was used to measure the complex permittivity and permeability of the CB-ABS composite filaments, where the mass ratio of CB and ABS is 1:7. The sample for the reflectivity test was fabricated via an FDM 3D printing machine (3D Raised E2, China). The reflectivity measurement was conducted in an arch free space measurement system. Detailed descriptions of the preparation, characterization and measurement are available in the supplementary material.

3. Results and discussion

3.1. Electromagnetic properties of the composite filaments

As shown in Fig. 2(a), the ε' and ε'' of CB-ABS composites decrease continuously with increasing frequency, which demonstrates its dispersion characteristics at different frequencies. According to the transmission line theory, the reflectivity of the single-layer flat structure was calculated. Figure 2(b) shows that the reflectivity peak gradually shifts towards the lower frequency with the increasing thickness. And we can discover that the single-layer flat structure cannot achieve broadband absorption.

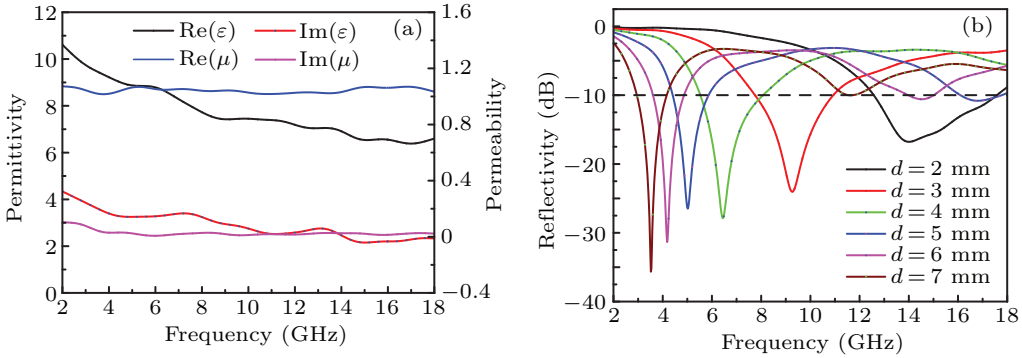


Fig. 2. (a) The ε and μ of CB-ABS composite; (b) the reflectivity of the single-layer flat structure.

3.2. Microwave absorbing properties of the dendritic fractal metamaterial

To obtain excellent electromagnetic wave absorption characteristics, the influence of the main geometric parameters (L, H, W, k, m, and t) was investigated. In Fig. 3(a), the lower border of the -10 dB absorbing bandwidth shifts from 9.3 GHz to 3.2 GHz with increasing H. The impact of H on reflectivity follows well the $\lambda/4$ resonance mechanism. Figure 3(b) shows a degree of attenuation of reflectivity intensity in middle and high frequencies when k increases from 0.6 to 1, while the absorption performance is significantly enhanced in the lower frequencies. Figures 3(c) and 3(d) depict the effective bandwidth is insensitive to W and m, while the reflectivity intensity in the lower frequency band strengthens first and then weakens with increasing W and m. Meanwhile, the change pattern of reflectivity intensity in the relative middle and high frequency band is contrary to the lower frequencies. Figures 3(e) and 3(f) show the reflectivity peak in the low frequency band moving towards higher frequencies with increasing L and t. Integrating the absorption bandwidth and reflectivity intensity, the optimal structural parameter combination for the GDFMs was confirmed as $H = 7$ mm, $W = 3.6$ mm, $L = 8$ mm, $k = 0.9$, $m = 0.5$, $t = 0.6$ and $D = 2$ mm.

As shown in Fig. 4(a), the microwave absorption characteristics of simulated and experimental results were compared and analyzed. The simulated microwave absorption of the GDFMs achieves -10 dB absorption bandwidth in the frequency range of 5.2–40 GHz, while the experimental sample in Fig. 4(b) could achieve a broadband absorption spectrum of 4.5–40 GHz. Though there exists a difference between the simulated and experimental results, the general behavior agrees well. The deviations mainly originate from manufacturing and measurement errors. Firstly, the discrepancy may be caused by unavoidable inconsistencies between the actual electromagnetic parameters and the simulation settings. The deformation of the fabricated structure in the 3D printing pro-

cess will also contribute to some degree of inaccuracy. Furthermore, due to the limitations of the measurement system, we measured reflectivity with an incident angle of 5° instead of the normal incidence angle.

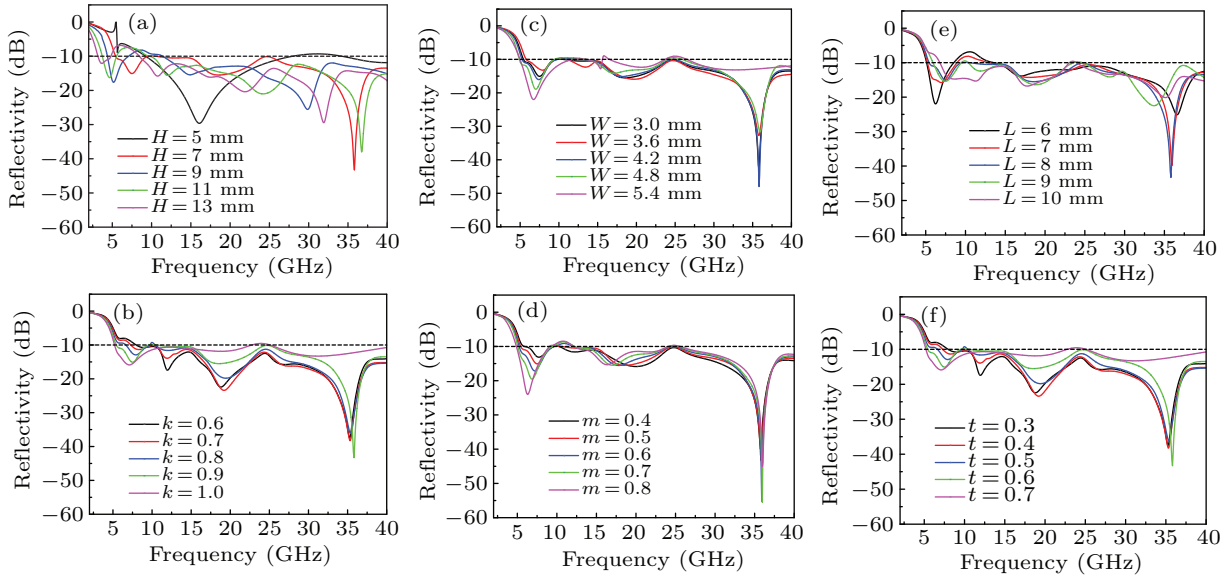


Fig. 3. Influence of the structural parameters on the absorption properties in the frequency range of 2–40 GHz: (a) H, (b) k, (c) W, (d) m, (e) L, and (f) t.

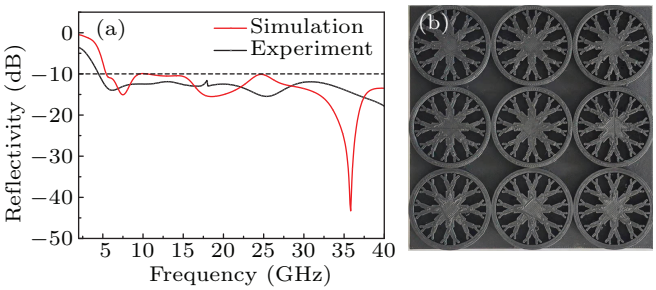


Fig. 4. (a) Comparison of simulation and experimental results; (b) the sample fabricated by FDM.

It is clear that the proposed GDFMs has relatively broadband absorption characteristics with a small thickness compared with other related devices which do not contain magnetic materials. Compared with the devices containing magnetic material, the GDFMs has a lower mass density under similar absorption performance. It can be concluded that the GDFMs is highly competitive with other metamaterial structures due to its great broadband absorption, thin thickness and light weight.

Table 1. Comparison of the proposed GDFMs with other related devices.

Structure	Bandwidth (−10 dB, GHz)	Thickness (mm)	Magnetic material	Reference
Swastika shape	9.3–49	3.6	No	[1]
Honeycomb structure	8.5–10.7, 11.9–18	12	No	[8]
Two-layer honeycomb sandwich structure	4.9–18	9	Yes	[10]
Gradient multilayer structure	5.1–40	10	Yes	[14]
Multilayer structure	8.2–18	20	Yes	[16]
Pyramid structure	2–2.36, 6.54–19.36, 19.89–21. 57, 25.1–40	7	Yes	[17]
Woodpile structure	4.5–40	5.6	No	[26]
Gradient dendritic fractal structure	4.5–40	7	No	this work

3.3. Dependence of polarization angle and oblique incidence

The performance of polarization-independent absorption is proved in Fig. 5(a), which results from the rotation symmetry of the GDFMs. As shown in Figs. 5(b) and 5(c), the reflectivity of different oblique incident angles is also numerically simulated. For TE polarization, as the incident angle increases from 0° to 50°, the absorption intensity decreases slightly. While the incident angle exceeds 50°, the absorption performance deteriorates rapidly. For TM polarization, the effect of oblique incident angle on the absorption performance is relatively slight. Even when the incident angle increases to 75°, the GDFMs could exhibit broadband absorption with an efficiency of over 90%. It can be concluded that the GDFMs

has a wide-angle absorption feature for both TE and TM polarization.

The strength of the magnetic field along the metamaterial surface has a significant impact on the wave absorption performance. For TE polarization, the incident angle gradually increases, resulting in a gradual decrease in the magnetic field component, while the situation under TM polarization is the exact reverse. Therefore, the change of the incident angle has little effect on the absorption performance of the electromagnetic wave in the TM mode.

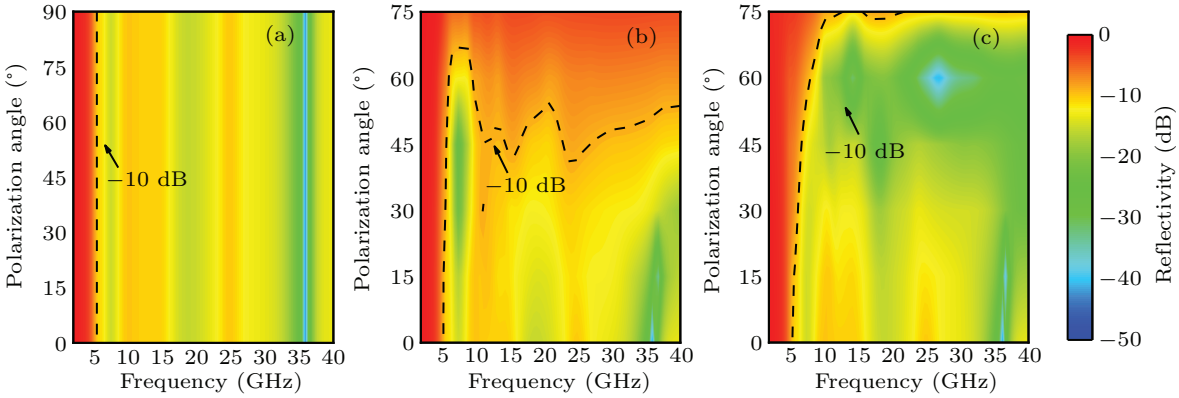


Fig. 5. The dependences of polarization angle (a) and oblique incidence of TE (b) and TM (c) polarization.

3.4. Absorption mechanism

In order to analyze the absorption mechanism of the GDFMs, the electric and magnetic field and power loss distributions at three reflectivity peaks were investigated. Figure 6(a) shows that the electric field mainly concentrates on the top layer of adjacent units in the x–z plane at the first frequency point of 7.5 GHz, while the magnetic field mainly concentrates on the bottom of the GDFMs in the y–z plane. The power loss concentrates on the outer circular structure and the bottom of the dendritic structure, overlapping the magnetic field distribution. This result indicates that the power loss at 7.5 GHz mainly derives from magnetic loss according to the $\lambda/4$ resonance.[27,28] When the frequency increases to 18.5 GHz, as shown in Fig. 6(b), the electric field energy is enhanced, especially on the top surface area. The magnetic field distribution shifts to the upper part of the GDFMs in the y–z plane, while partial magnetic field energy is distributed at the junction of the dendritic structure. The power loss at the center of the GDFMs is enhanced, which is similar to the magnetic field. It reveals that the power loss at 18.5 GHz is mainly attributed to strong resonance and weak edge diffraction.[14,29] At the third frequency point of 35.8 GHz, as shown in Fig. 6(c), the electric and magnetic field both concentrate on the top edge area of the top layer and the gap between the units. The power loss distribution at the top edges of the GDFMs is identical to the electric and magnetic field distributions. And the power loss is also distributed in the gaps between the unit structures. This result indicates that the power loss at 35.8 GHz is mainly attributed to strong edge diffraction and weak resonance.[17]

In summary, through the analysis of electromagnetic field and power loss distributions, it could be concluded that the excellent broadband absorption characteristics of the GDFMs is mainly attributed to the magnetic loss in the bottom layer, the resonance between adjacent units and the branches of the gradient dendritic structure, and the edge diffraction effects at the edges of the top layer.

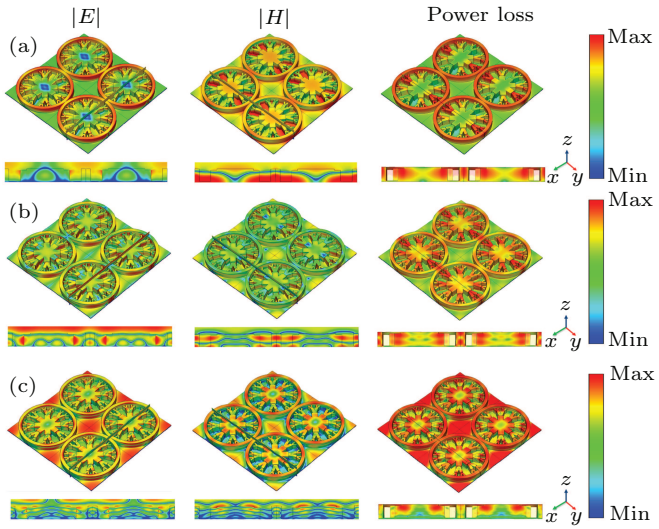


Fig. 6. Distributions of the electric field, magnetic field and power loss of the GDFMs at three reflectivity peaks: (a) 7.5 GHz; (b) 18.5 GHz; (c) 35.8 GHz.

As we all know, when the metamaterial structure is confirmed, it will generate resonance to strengthen the electromagnetic wave absorption at some fixed frequency positions. The previously reported metamaterial structures usually generate resonance by the structural design in the vertical or horizontal directions for electromagnetic wave absorption. The proposed three-dimensional dendritic structure in this paper has more structural features, which can generate more resonance points to achieve broadband absorption. Furthermore,

the combination of gradient design and dendritic fractal structure will produce more edge structural features, which will significantly enhance the structural resonance and edge diffraction effects.

4. Conclusion and perspectives

The GDFMs based on CB-ABS was numerically and experimentally demonstrated to show broadband absorption characteristics. Furthermore, the GDFMs is insensitive to polarization and incident angle. Compared with the flat structure, the proposed GDFMs not only significantly increases the effective bandwidth, but also improves the material utilization. It is believed that this study could provide a novel and viable strategy for designing and fabricating lightweight broadband absorbing metamaterial in the future.

Acknowledgements

Project supported by the Natural Science Foundation of Shaanxi Province of China (Grant No. 2022JQ-356), the Youth Fund of Rocket Force University of Engineering (Grant No. 2022QN-B017), and the National Natural Science Foundation of China (Grant No. 51905542).

References

[1] Zhang X F, Zhang D J, Fu Y J, Li S H, Wei Y, Chen K J, Wang X and Zhuang S L 2020 *IEEE Antenn. Wirel. Pr.* **19** 821
[2] Mei H, Zhao X, Zhou S X, Han D Y, Xiao S S and Cheng L F 2019 *Chem. Eng. J.* **372** 940
[3] Yang Z, Liang Q X, Duan Y B, Li Z H, Li D C and Cao Y 2021 *Compos. Struct.* **274** 114330
[4] Zhang K L, Hou Z L, Bi S and Fang H M 2017 *Chin. Phys. B* **26** 127802
[5] Luo W J, Yan S and Zhou J 2022 *Interdiscip. Mater.* **1** 11
[6] Zhang F L, Li C, Fan Y C, Yang R S, Shen N H, Fu Q H, Zhang W H, Zhao Q, Zhou J, Koschny T and Soukoulis C M 2019 *Adv. Mater.* **31** 1903206
[7] Mei H, Yang W Q, Zhao X, Yao L, Yao Y T, Chen C and Cheng L F 2021 *Mater. Des.* **197** 109271
[8] Sheng J Q, Zhang Y, Liu L, Quan B, Zhang N and Ji G B 2019 *J. Alloys Compd.* **809** 151866
[9] Zhang N, Gu W H, Zhao Y, Zheng J, Pei C C, Fan F Y and Ji G B 2021 *J Mater Sci: Mater Electron* **32** 25809
[10] Luo H, Chen F, Wang X, Dai W Y, Xiong Y, Yang J J and Gong R Z 2019 *Compos. Part A-Appl. S* **119** 1
[11] Li M L, Muneer Badar, Yi Z X and Zhu Q 2018 *Adv. Opt. Mater.* **6** 1701238
[12] Zhang Y, Huang Y, Zhang T F, Chang H C, Xiao P S, Chen H H, Huang Z Y and Chen Y S 2015 *Adv. Mater.* **27** 2049
[13] Xu J, Fan Y C, Su X P, Guo J, Zhu J X, Fu Q D and Zhang F L 2021 *Opt. Mater.* **113** 110852
[14] Duan Y B, Liang Q X, Yang Z, Li Z H, Yin H Y, Cao Y and Li D C 2021 *Mater. Des.* **208** 109900
[15] Zhou Q, Yin X W, Ye F, Liu X F, Cheng L F and Zhang L T 2017 *Mater. Des.* **46** 1
[16] Yang D, Yin Y F, Zhang Z K, Li D C and Cao Y 2020 *Mater. Lett.* **281** 128571
[17] Huang Y, Song W L, Wang C, Xu Y, Wei W, Chen M, Tang L and Fang D 2018 *Compos. Sci. Technol.* **162** 206
[18] Xiong Y J, Wang Y, Wang Q, Wang C Q, Huang X Z, Zhang F and Zhou D 2018 *Acta Phys. Sin.* **67** 084202 (in Chinese)
[19] Fu T, Liu X X, Wen G H, Sun T Y, Xiao G L and Li H O 2021 *Chin. Phys. B* **30** 14201
[20] Cheng Y Z, Luo H and Chen F 2020 *J. Appl. Phys.* **127** 214902
[21] Wen Y Z, Ma W, Bailey J, Matmon G and Yu X M 2015 *IEEE Trans. THz Sci. Technol.* **5** 406
[22] Wang T, He H H, Ding M D, Mao J B, Sun R and Sheng L 2022 *Chin. Phys. B* **31** 37804
[23] Xu H X, Wang G M, Tao Z and Cui T J 2014 *Sci. Rep.* **4** 5744
[24] Zhou D, Huang X Z and Du Z J 2017 *IEEE Antenn. Wirel. Pr.* **16** 133
[25] Saptarshi G and Sungjoon L 2018 *IEEE Antenn. Wirel. Pr.* **17** 2379
[26] Yin L X, Tian X Y, Shang Z T and Li D C 2019 *Mater. Lett.* **239** 132
[27] Jia W, Ren P W, Tian Y C and Fan C Z 2019 *Chin. Phys. B* **28** 26102
[28] Zhang J M, He D L, Wang G W, Wang P, Qiao L, Wang T and Li F S 2019 *Chin. Phys. B* **28** 58401
[29] Yang R S, Xu J, Shen N H, Zhang F L, Fu Q H, Li J J, Li H Q and Fan Y C 2021 *InfoMat* **3** 577